Vertically oriented MoS_2 nanosheets with vast exposed edges for enhanced electrocatalytic hydrogen evolution

Meisheng Han[1,3], Jie Yu[1,2*]

[1]Songshan Lake Materials Laboratory Dongguan, Guangdong, 523808, China
[2]Shenzhen Engineering Lab for Supercapacitor Materials, Shenzhen Key Laboratory for Advanced Materials, School of Material Science and Engineering, Harbin Institute of Technology, Shenzhen, University Town, Shenzhen, 518055, China
[3]Beijing National Laboratory for Condensed Matter Physics, Institute of Physics, Chinese Academy of Sciences, Beijing, 100190, China

Abstract. Molybdenum disulfide (MoS_2), a typical two-dimensional transition metal dichalcogenides, is a promising candidate for electrochemical water splitting catalysis due to its ultrahigh special area and highly exposed active edge sites. The main challenges restricted the wider application for MoS_2-based nanomaterials are the complex preparation process and the high overpotential. Here, we design a novel and facile sealed vessel to synthesize vertical oriented MoS_2 nanosheets electrocatalyst with vast exposed edges. Benefiting from the unique vertically-oriented structural and compositional characteristics, the MoS_2 nanosheets with 10-20 layers exhibits superior hydrogen evolution reaction (HER) performance with a small overpotential of 135.2 mV at a current density of 10 $mA \cdot cm^{-2}$ and low Tafel slope of 82.5 $mV \cdot dec^{-1}$ as well as extraordinary catalytic stability over 5000 cycles. Importantly, the sealed vessel reactor system may open up a versatile and potential synthetic way to construct various morphologies and structure of metal dichalcogenides for high-performance energy storage and conversions devices.

1 Introduction

2D layered transition metal dichalcogenides (TMDCs) owing to their exciting electrochemical and optoelectronic properties, which have inspired a broad range of fundamental and practical interests in electrochemical energy storage and conversion as well as optoelectronic device [1, 2]. Particularly, MoS_2 has emerged as a new possibility beyond commercial 20 wt% Pt/C catalyst in facilitating efficient electrochemical hydrogen evolution [3, 4]. However, like many other metal sulfides-based catalysts, MoS_2-based catalysts are still plagued with two main challenges: the complicated synthesis process and high overpotential caused by a small quantity active edge sites and the low intrinsic electric conductivity, impede its broad range of applications [3]. Up to now, Pt-based electrocatalysts exhibit most excellent electrocatalytic activity, but the scarcity and high-cost seriously restricted their widespread applications [5, 6]. Therefore, the research for an earth-abundant, high catalytic activity and commercial water-splitting MoS_2-based electrocatalyst is still imperative.

For this purpose, enormous synthetic method and strategies have been explored to design and midificate catalytic functionality of MoS_2. One of the major synthesis methods is chemical vapour deposition (CVD) [7], which can effectively control morphological of MoS_2, introduce sulfur vacancy sites and strain or disorder [8]. However, the use of H_2S or H_2/N_2 forming gas always cause environmental pollution and resource waste in an open system. Moreover, additional electronic and structural modification always need high precision experimental equipment. Another major strategy is solution-processed approaches [9], which can engineer various morphologies and structure of MoS_2 to enhance their intrinsic activity and conductivity by atomic-scale engineering [10] or coupling with conductive substrate, such as carbon nanosheet [11], carbon nanotube [12], graphene [13], or 3D metals [14]. Whereas, it still needs to be pointed out that solution-processed approaches is normally complicated, uncontrollable and require multiple process [15]. In addition to, electrodeposition is also an important strategy. For example, Kibsgaard [16] et al. engineered MoS_2 mesoporous films with double-gyroid via template-assisted electrodeposition to maximally expose active edge sites due to the existence of the predominant inert (0001) basal plane with relatively larger Gibbs free energy [8]. Nevertheless, removing the template may influence the structure of MoS_2. Therefore, seeking to simple and high-yield approaches to synthesize hierarchical MoS_2-based nanomaterial is requisite [17,18].

Here, we design a novel and facile sealed vessel to synthesize MoS_2-based nanostructures and investigate their electrocatalytic performance. The sealed vessel is a significant and attractive synthetic method due to its one-step preparation via mixed precursors without organic solvents or toxic gases. By virtue of sealed vessel, we first have designed and synthesized vertically oriented

* Corresponding author: jyu@hit.edu.cn

MoS_2 nanosheets with enormous exposed edges, which exhibits remarkable electrochemical performance with small Tafel slope of 82.5 $mV \cdot dec^{-1}$ and an overpotential of 135.2 mV at a current density of 10 $mA \cdot cm^{-2}$ as well as extraordinary catalytic stability over 5000 cycles.

2 Experimental

2.1 Preparation of MoS_2 nanosheets

The overall synthesis approach involves the following steps. In brief, first, all reaction source were mixed with pestle for several minutes under ambient conditions where 0.2 g $H_3P(Mo_3O_{10})_4 \cdot xH_2O$ was used as the molybdenum source, and 0.3 g sulfur powder as the sulfur source. Subsequently, the mixed precursor was transferred into and sealed a homemade sealed vessel in the Ar-filled glove box. Finally, the sealed vessel was heated at 600 °C for 2 hours with a heating ramp rate of $10°C \cdot min^{-1}$ under inert atmosphere to obtain MoS_2 nanosheets. After the sealed vessel natural cooling to room temperature in the furnace, The final product was gained for further analysis.

2.2 Characterizations

Morphology was investigated field-emission scanning electron microscopy (Hitachi FESEM S-4700) equipped with EDS. Transmission electron microscopy (TEM, TECNAI G2 F20) was used to test the microstructures. The Raman was performed using Renishaw RW100 Micro-Raman system system with an excitation laser line of 514.6 nm in ambient air environment. Crystal structure of the materials was performed by a Grazing Incident Angle XRD (GIAXRD) with Cu Kα (λ = 0.154 nm) as the radiation source XRD (Bruker D2). The X-ray photoemission spectroscopy (XPS ESCALAB-250) equipped with Al (K-alpha) source was carried out to obtain the bonding information of the elements and Co doping contents.

2.2 Electrochemical measurements

Electrochemical measurements were performed with an electrochemical analyzer (CHI760D) under ambient conditions. Rotation disk electrodes of grassy carbon (GC, PINE, 4 mm diameter) modified with different catalysts were rotated at 2000 rpm. In a typical modification process, the GC surface was polished to a mirror finishing followed by a thorough cleaning with H_2O in ultrasonication bath. 2 mg of the synthesized material were dispersed in mixed solvent: 360 μL water-ethanol (v:v=3:1) and 40 μL Nafion solution (5wt%) followed by ultrasonincation for 120 min, forming a homogeneous suspension with a concentration of $5mg \cdot mL^{-1}$. 10 μL of catalyst dispersion was drop into a cleaned GC electrode with pipet and the solvent was evaporated at room temperature (≈0.40 $mg \cdot cm^{-2}$). In the measurement, the modified GC electrodes were acted as working electrode with a graphite rod as counter electrode, and Ag/AgCl (3 M KCl) as reference electrode in the three-electrode electrochemical cell. An aqueous solution of 0.5 M H_2SO_4 with a pH value of 0.1 was used as electrolyte and purged with N_2 gas for at least 30 min before measurements. The HER performance was investigated using linear sweep voltammetry (LSV) under potentials between 0.1 and -0.6 V versus RHE at the scan rate of 5 $mV \cdot s^{-1}$. The stability of catalysts was examined by consecutive LSV scans over 5000 cycles. All the data here were collected without iR compensation and all the potentials were calibrated with respect to a RHE by the equation E (vs. RHE) = E^0 (Ag/AgCl)+E (vs. Ag/AgCl) +0.059PH.

3 Results and discussion

Figures 1 displays the SEM image of the obtained MoS_2, and it can be found that vertically oriented MoS_2 nanosheets with vast exposed edges are obtained.

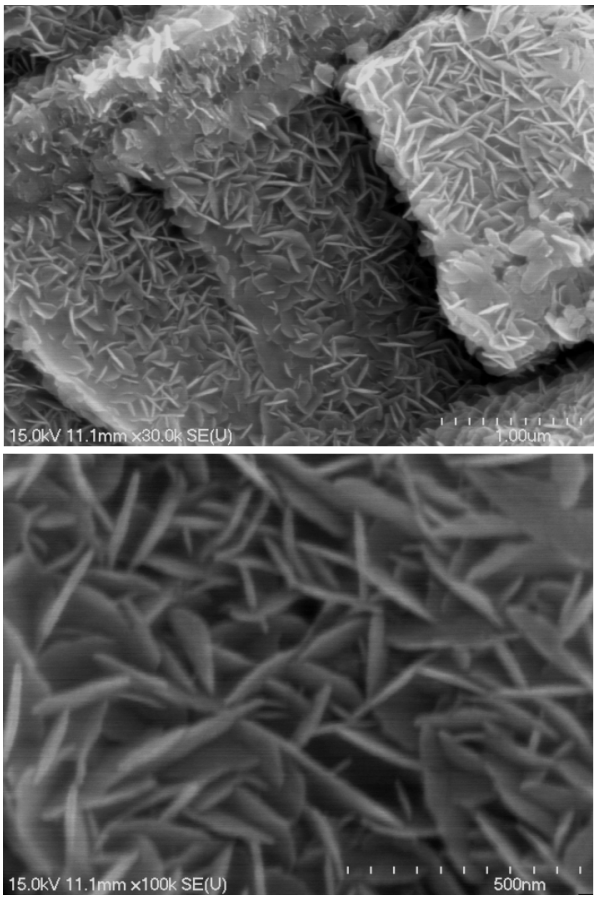

Figure 1. SEM images of the obtained sample.

The TEM and high-resolution TEM images (Figure 2) show that the MoS_2 nanosheets possess the layer number of 10-20. So thin nanosheets are favorable for the exposure of active sites.

Figure 3a shows that all the identified peaks can be uniquely indexed to a hexagonal phase of MoS_2 (JCPDS card no. 37-1492). The Raman spectrum (Figure 3b) shows two characteristic peaks located at 373.2 and 401.2 cm^{-1}, which are assigned to the E^1_{2g} and A_{1g} band of MoS_2 material, respectively. Figure 3c shows that the

peak positions of the Mo $3d_{3/2}$ and Mo $3d_{5/2}$ binding energies of Mo^{4+} are located around 232.18 and 228.87 eV, respectively. Figure 3d shows two peaks located at 163.49 and 162.29 eV for the S 2p XPS spectrum, corresponding to the characteristic peaks of S $2p_{1/2}$ and S $2p_{3/2}$, respectively. The above results fully demonstrate the formation of hexagonal MoS_2.

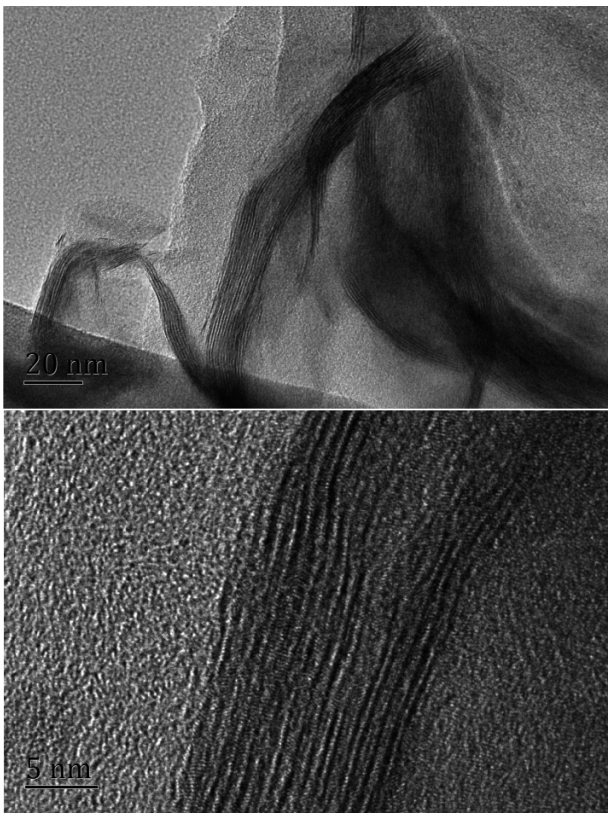

Figure 2. TEM images of the obtained sample.

Figure 4a shows the typical cathodic polarization curve of MoS_2 nanosheets, which shows a small overpotential of only 135.2 mV at the current density of 10 $mA \cdot cm^{-2}$. To understand the detailed underlying mechanism of HER activity of catalysts, Tafel plots curves are acquired, as shown in Figure 4b, which shows a small Tafel slope of ~ 82.5 $mV \cdot dec^{-1}$ and indicates its HER mechanism follows Volmer-Heyrovsky reaction where electrochemical desorption is the rate-determining step. To further evaluate the stability of the catalysts, consecutive LSV scans are carried out. As shown in Figure 4c, after 5000 cycles, the LSV curves show very small shifts, further demonstrating the high stability of the obtained electrocatalysts.

The excellent HER performance may be attributed to the few-layered and the vertically oriented nanostructure, which can expose more active sites, decrease the distance of electron transfer, and well maintain the material stability.

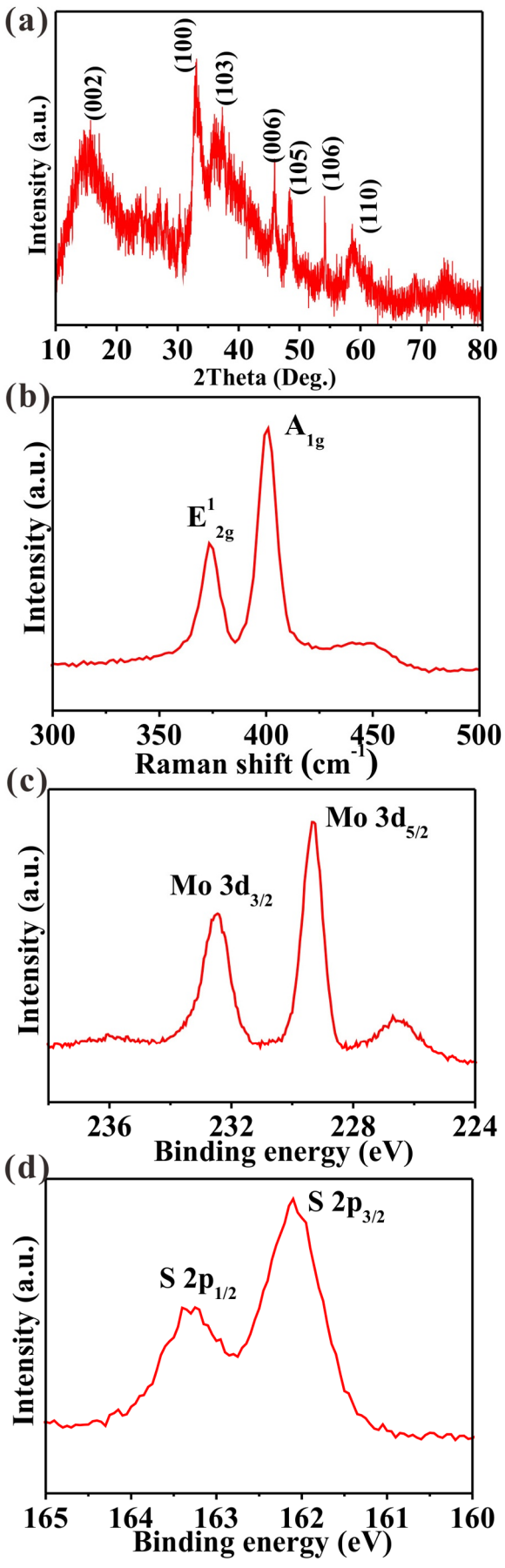

Figure 3. (a) XRD pattern, (b) Raman spectrum, (c) Mo 3d, (d) S 2p of the obtained MoS_2.

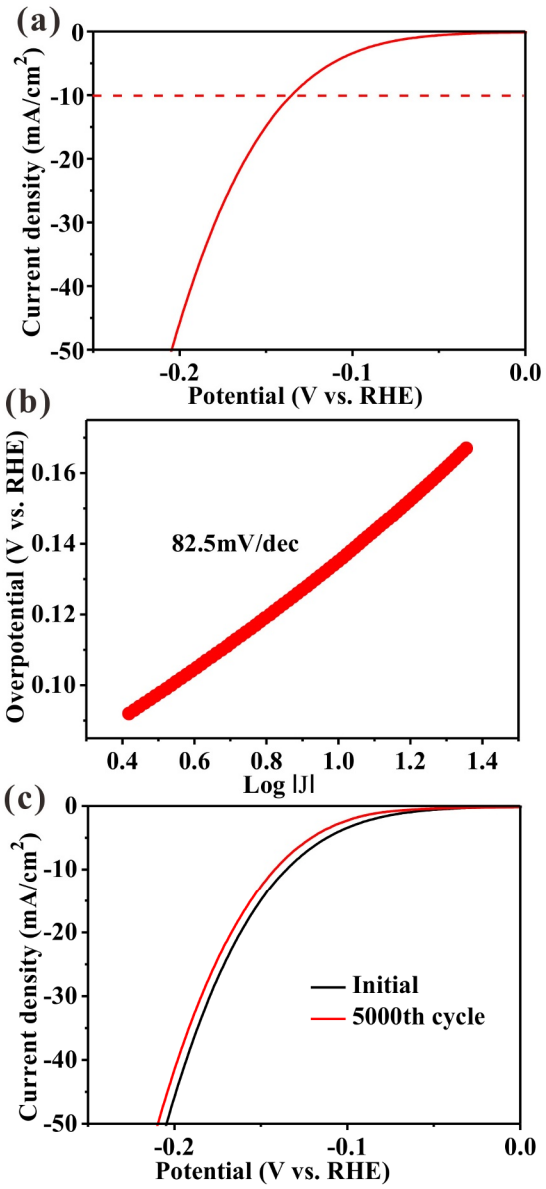

Figure 4. Electrochemical catalytic activities of MoS_2 nanosheets for hydrogen evolution. (a) LSV curve, (b) Tafel plots, (c) LSV curves during cycling.

4 Conclusions

Here, we have designed a novel hermetic container to one-step synthesize vertically oriented MoS_2 nanosheets with vast exposed edges. As expected, as HER electrocatalysts, the MoS_2 nanosheets exhibit remarkable electrochemical performance with high current density, low Tafel slope, and persistent stability in acid solution. The dramatically improved electrocatalytic performance of the MoS_2 nanosheets is attributed to its unique structure, such as vertically orientation, few-layered structure, and vast exposed edges. Importangtly, Compared to other synthetic approach, the method with hermetic sealed vessel is facile and easily reproducible for synthesizing the MoS_2 nanosheets by utilizating low-cost precursors, which could be extended to other materials for better large-scale production of electrochemical energy storage and conversions devices.

Acknowledgements

Meisheng Han acknowledges support from Guangdong Basic and Applied Basic Research Foundation (2020A1515110762).

Thank for technical support from “Ceshigo Research Service agency for TEM, “www.ceshigo.com”.

Thank Eric Zhang from ZhongKe BlueOcean (TianJin) Technology Co.,Ltd (www.zkbotj.com) for XRD analysis.

Thank Jiaojiao Fang from Shiyanjia Lab (www.shiyanjia.com) for the SEM analysis.

References

1. Y. Chen, Z. Li, U. Paik, X. (David) Lou, Sci. Adv. **2**, 1600021 (2016).
2. X. Cao, C. Tan, X. Zhang, W. Zhao, H. Zhang, Adv. Mater. **28**, 6167-6696 (2016).
3. Y. Cheng, S. Lu, F. Liao, L. Liu, Y. Li, M. Shao, Adv. Funct. Mater. **27**, 1700359-1700366 (2017).
4. M. Gao, J. Liang, Y. Zheng, Y. Xu, J. Jiang, Q. Gao, J. Li, S. Yu, Nat. Commun. **6**, 5982-5988 (2015).
5. R.T. D. Subbaraman, D. Strmcnik, K. Chang, M. Uchimura, A. P. Paulikas, V. Stamenkovic, N. M. Markovic, Sci. **334**, 1256-1260 (2011).
6. P. Wang, K. Jiang, G. Wang, J. Yao, Angew. Chem. Int. Ed. **55**, 12859-12863 (2016).
7. G. W.Shim, W.H. Sang, Y. Yang, S.-Y. Cho, J. Mater. Chem. A. **5**, 14950-14968 (2017).
8. H. Li, C. Tsai, A. L. Koh, L. Cai, A. W. Contryman, A. H. Fragapane, J. Zhao, H. S. Han, H. C. Manoharan, F. Abild-Pedersen, J. K. Nørskov, X. Zheng, Nat. Mater. **15**, 364-368 (2016).
9. X.Y. Yu, L. Yu, X.W.D. Lou, Small Methods, **1**, 1600020-1600028 (2017).
10. J. Miao, F. Xiao, H. Yang, Sci. Adv. **1**, 1500259 (2015).
11. L. Yang, W. Zhou, J. Lu, D. Hou, Nano Energy **22**, 490-498 (2016).
12. J. Ekspong, T. Sharifi, A. Shchukarev, A. Klechikov, W. Thomas, E. Gracia-Espino, Adv. Funct. Mater. **26**, 6766-6776 (2016).
13. Y. Su, F .Alimohammadi, D. Zhang, G. Guo, Nano Lett. 17, 1963-1969 (2017).
14. T. Wang, L. Liu, Z. Zhu, P. Papakonstantinou, J. Hu, H. Liu, M. Li, Energy Environ. Sci. **6**, 625-633 (2013).
15. X. Zhang, Z. Lai, C. Tan. Angew. Chem. Int. Ed. **55**, 8816-8838 (2016).
16. J. Kibsgaard, Z. Chen, B. N. Reinecke, T. F. Jaramillo, Nat. Mater. **11**, 963-969 (2012).

17. Z. Gong, H. Liu, J. Qu, J. Li. Energy Environ. Sci. **9**, 1190-1209 (2016).
18. X. Yu, Y. Feng, Y. Jeon, B. Guan, X. Wen, Adv. Mater. **28**, 9006-9011 (2016).